

UC Riverside

Previously Published Works

Title

Comparison of Vehicle Exhaust Particle Size Distributions Measured by SMPS and EEPS During Steady-State Conditions

Permalink

<https://escholarship.org/uc/item/3933d6cn>

Journal

Aerosol Science and Technology, 49(10)

ISSN

0278-6826 1521-7388

Authors

Xue, Jian
Li, Yang
Wang, Xiaoliang
[et al.](#)

Publication Date

2015-09-01

DOI

10.1080/02786826.2015.1088146

Peer reviewed





Comparison of Vehicle Exhaust Particle Size Distributions Measured by SMPS and EEPs During Steady-State Conditions

Jian Xue, Yang Li, Xiaoliang Wang, Thomas D. Durbin, Kent C. Johnson, Georgios Karavalakis, Akua Asa-Awuku, Mark Villela, David Quiros, Shaohua Hu, Tao Huai, Alberto Ayala & Heejung S. Jung


To cite this article: Jian Xue, Yang Li, Xiaoliang Wang, Thomas D. Durbin, Kent C. Johnson, Georgios Karavalakis, Akua Asa-Awuku, Mark Villela, David Quiros, Shaohua Hu, Tao Huai, Alberto Ayala & Heejung S. Jung (2015) Comparison of Vehicle Exhaust Particle Size Distributions Measured by SMPS and EEPs During Steady-State Conditions, *Aerosol Science and Technology*, 49:10, 984-996, DOI: [10.1080/02786826.2015.1088146](https://doi.org/10.1080/02786826.2015.1088146)

To link to this article: <https://doi.org/10.1080/02786826.2015.1088146>

 View supplementary material [↗](#)

 Accepted author version posted online: 01 Sep 2015.
Published online: 22 Sep 2015.

 Submit your article to this journal [↗](#)

 Article views: 1768

 View Crossmark data [↗](#)

 Citing articles: 22 View citing articles [↗](#)



Comparison of Vehicle Exhaust Particle Size Distributions Measured by SMPS and EEPs During Steady-State Conditions

Jian Xue,^{1,2} Yang Li,^{1,2} Xiaoliang Wang,³ Thomas D. Durbin,¹ Kent C. Johnson,¹ Georgios Karavalakis,¹ Akua Asa-Awuku,¹ Mark Villela,¹ David Quiros,⁴ Shaohua Hu,⁴ Tao Huai,⁴ Alberto Ayala,⁴ and Heejung S. Jung^{1,2}

¹Center for Environmental Research and Technology (CE-CERT), Bourns College of Engineering, University of California–Riverside (UCR), Riverside, California, USA

²Department of Mechanical Engineering, University of California–Riverside (UCR), Riverside, California, USA

³Desert Research Institute, Reno, Nevada, USA

⁴California Air Resources Board (CARB), Sacramento, California, USA

Fast-sizing spectrometers, such as the TSI Engine Exhaust Particle Sizer (EEPS), have been widely used to measure transient particle size distributions of vehicle exhaust. Recently, size distributions measured during different test cycles have begun to be used for calculating suspended particulate mass; however, several recent evaluations have shown some deficiencies in this approach and discrepancies relative to the gravimetric reference method. The EEPs converts electrical charge carried by particles into size distributions based on mobility classification and a specific calibration, and TSI recently released a matrix optimized for vehicle emissions as described by Wang et al. (Submitted). This study evaluates the performance of the new matrix (soot matrix) relative to the original matrix (default matrix) and reference size distributions measured by a scanning mobility particle sizer (SMPS). Steady-state particle size distributions were generated from the following five sources to evaluate exhaust particulates with various morphologies estimated by mass-mobility scaling exponent: (1) A diesel generator operating on ultralow sulfur diesel, (2) a diesel generator operating on biodiesel, (3) a gasoline direct-injection vehicle operating at two speeds, (4) a conventional port-fuel injection gasoline vehicle, and (4) a light-duty diesel (LDD) vehicle equipped with a diesel particulate filter. Generally, the new soot matrix achieved much better agreement with the SMPS reference for particles smaller than 30 nm and larger than 100 nm, and also broadened the accumulation mode distribution that was previously too narrow using the default matrix. However, EEPs distributions still did not agree with SMPS reference measurements when challenged by a strong nucleation

mode during high-load operation of the LDD vehicle. This work quantifies the range of accuracy that can be expected when measuring particle size distribution, number concentration, and integrated particle mass of vehicle emissions when using the new static calibration derived based on the properties of classical diesel soot.

1. INTRODUCTION

Mobile source emissions, contributing significantly to urban particle pollution, are linked with cardiovascular and pulmonary diseases (Donaldson et al. 1998; Oberdorster et al. 2004), and therefore present widespread environmental problems. In January 2012, the California Air Resources Board (CARB 2012) adopted the Low Emissions Vehicle (LEV) III regulations, which lowered the particulate matter (PM) emission standards over the Federal Test Procedure (FTP) for light-duty vehicles (LDVs) from 10 mg/mile to 3 mg/mile beginning with the model year (MY) 2017, and to 1 mg/mile beginning with MY 2025. The US Environmental Protection Agency (USEPA 2013) also has enacted the Tier 3 Vehicle Emission and Fuel Standards Program, which lowers PM emission standards for LDVs to 3 mg/mile beginning in MY 2017. With the advances in engine technologies resulting in lower PM emissions, there is need to continue to explore improvements and alternatives to measuring PM mass at very low levels.

Current regulations for motor vehicle PM emissions in the United States are based on gravimetric determination of PM that is collected onto filter media as defined by Code of Federal Regulations (CFR), parts 1065 and 1066. One of the alternative PM measurement methods that CARB (2012) is evaluating to support the LEV III PM standards is integrated particle size distribution (IPSD) (Liu et al. 2009), which

Received 3 October 2014; accepted 31 July 2015.

Address correspondence to Heejung S. Jung, Center for Environmental Research and Technology (CE-CERT), Bourns College of Engineering, University of California–Riverside (UCR), A357 Bourns Hall, 900 University Avenue, Riverside, CA 92521, USA. Email: heejung@engr.ucr.edu

Color versions of one or more figures in this article can be found online at www.tandfonline.com/uast.

estimates real-time suspended particle mass from particle size distribution (PSD) and an effective density function. Since the method does not use filter media, IPSD is unaffected by gaseous adsorption artifact or particle evaporation after collection onto filters, and therefore has been explored to evaluate whether the method offers greater sensitivity for measuring PM mass at low emission levels (Liu et al. 2009; Li et al. 2014; Quiros et al. 2015a). Furthermore, measuring PSD provides not only the ability to estimate PM mass but also other important characteristics of vehicle particle emissions such as total particle number and surface area.

Suspended particle mass in motor vehicle emissions has also been evaluated using other types of real-time instruments. Maricq et al. (2006) reported the estimation of suspended PM mass using an Electrical Low Pressure Impactor (ELPI; Dekati Ltd., Kangasala, Finland). The EPLI measures real-time aerodynamic PSDs using cascade low-pressure impactors and electrometers at each stage. Although aerodynamic distributions require no knowledge of particle density to obtain an accurate mass distribution, particle charging efficiency depends on particle mobility diameter and shape but not aerodynamic diameter, and thus the accuracy of the size distributions reported by the ELPI may vary depending on particle morphology. Considering these fundamental and other experimental uncertainties, Maricq et al. (2006) estimated that the integration of aerodynamic size distributions using the ELPI yielded an uncertainty of about 20% in quantifying vehicle exhaust PM mass. Later, Dekati Ltd. developed the Dekati Mass Monitor (DMM) that, among other improvements for measuring engine exhaust, combines aerodynamic and mobility classifications to determine particle effective density in real-time by assuming a unimodal distribution (Lehmann et al. 2004). Mamakos et al. (2006) showed that the DMM overestimates PM mass from 3 to 40% over transient cycles. Due to the “black-box” operation of the DMM, which uses a proprietary method for calculating particle effective density and size distribution, the authors and several other groups have been unsuccessful in unequivocally pinpointing the source of error or discrepancy. Another instrument that does not measure particle size, the Micro Soot Sensor (MSS; AVL, Graz, Austria) is frequently used to quantify real-time particle mass (Khalek et al. 2010) using photo-acoustic signals to detect black carbon that is assumed to linearly correlate with filter-based gravimetrically determined particle mass. While the instrument is sensitive to PM mass at low levels, it does not detect the non-light absorbing fraction of PM. Accordingly, Silvis (2012) reported a method that can estimate non-light absorbing fraction of vehicle PM, such as the Soluble Organic Fraction (SOF), along with the MSS signal at certain conditions, so that MSS can be used to quantify vehicle exhaust PM mass, including the non-light absorbing fraction. This method does not actually measure, and instead estimates the SOF fraction, and therefore the accuracy of

this approach is insufficient for regulatory PM mass determination.

The Scanning Mobility Particle Sizer (SMPS) is widely accepted as a reference instrument for measuring PSD in the submicron range (Wang and Flagan 1990; Mulholland et al. 2006). It provides high size resolution (100 channels from 2 to 1000 nm) with a reported size accuracy within 3% for spherical particles (Kinney and Pui 1991). However, the SMPS requires at least 1 min to scan the entire particle size range and is not suitable for measuring transient vehicle exhaust emissions. Shah and Cocker (2005) initially developed a fast SMPS to reduce this scan time down to 2.5 s, but only for the size range below 150 nm, which does not cover the full size range of interest for vehicle exhaust. The fastest commercially available SMPS from TSI Incorporation (Shoreview, MN, USA) requires a longer scan time of approximately ~10 s, and is therefore also not suitable for measuring PSDs during transient cycles.

Other instruments, such as the TSI Engine Exhaust Particle Sizer (EEPS; 5.6–560 nm) (Johnson et al. 2003, 2004; TSI 2013) can measure emissions over a suitable range and at high time resolution (10 Hz). Early developments by Mirme (1994) at Tartu University and Biskos et al. (2005), led to the commercialized systems available today, such as the EEPS by TSI and the DMS500 by Cambustion. In recent years, both the EEPS and DMS500 have been widely used for emission measurement and characterization (Liu et al. 2005; Rubino et al. 2005; Yao et al. 2006; Zervas and Dorlhene, 2006; Zheng et al. 2012). The two instruments have multiple electrometers downstream of a corona charger to measure size distributions. The inversion of electrometer current measured at multiple electrometers into a size distribution requires an instrument matrix that accounts for particle charge distribution and a transfer function for mobility classification. The EEPS instrument matrix comprises 22 rows and 17 columns, with each column representing the electrical current measured by 22 electrometers when the EEPS is challenged by a unit concentration of mono-disperse particles with a central diameter of one of the 17 primary bin sizes (Wang et al. Submittedb).

The initial EEPS matrix (default matrix) that has been widely used over the past decade was developed based on theoretical calculations and experimental evaluations using a prototype EEPS with near-spherical particles (e.g., oil droplets, sodium chloride, and polystyrene latex spheres [PSL]) (Wang et al. Submittedb). As more data became available from EEPS users, it became evident that the default matrix did not accurately report the size distribution for near-spherical particles, and discrepancies relative to reference methods, such as the SMPS, were even more severe when measuring soot particles characterized by more fractal morphologies (Rubino et al. 2005; Wang et al. 2009; Jeong and Evans, 2009; Asbach et al. 2009; Kaminski et al. 2013; Quiros et al. 2014). Generally, the EEPS agrees better with the SMPS for compact shape particles <~75 nm, such as NaCl aerosol, but much narrower

distributions are reported for EEPS when characterizing more fractal-like particles, such as diesel exhaust (Asbach et al. 2009; Kaminski et al. 2013; Zimmerman et al. 2014). Wang et al. (Submitteda) showed that the geometric mean diameters (GMDs) measured by EEPS agreed with those by SMPS within 15% for diesel engine exhaust particles <50 nm, but underestimated by 20–50% for larger particles. Zimmerman et al. (2014) attributed disagreement to different properties and morphology of the ambient and engine exhaust particles. In a unipolar charging environment, aggregates of fractal morphology carry more charge than near spherical particles of equivalent mobility diameter (Chang 1981) by 20–30% as shown experimentally by Shin et al. (2010) and Oh et al. (2004). Although some studies have proposed and demonstrated corrections for size distributions measured by the default matrix (Zimmerman et al. 2015; Quiros et al. 2014, 2015a), there is continued interest in deriving accurate size distributions directly from the instrument following.

A more fundamental approach to report accurate size distributions was developed by Wang et al. (2009), which accounted for differences in charge distribution among particles of different shapes. Rather than using a universal instrument matrix to characterize particles of all morphologies, two new matrices were created, and recently distributed commercially by TSI (2015): one for compact shape particles (compact matrix; Wang et al. Submittedb) and another for engine exhaust particles (soot matrix; Wang et al. submitted). The soot matrix was created using mono-disperse and poly-disperse particles from a John Deere 4045H diesel engine under steady-state operations. The emissions from this engine under similar conditions were previously reported to have a mass-mobility scaling exponent (D_m) ranging from 2.3 to 2.4 (Park et al. 2003), a range that coincides with the mass-mobility relationship of particulates emitted from many classifications of modern light- and heavy-duty engines. The mono-disperse particles (10–400 nm) were used to update the relationship between particle size/concentration and electrometer number/current. The polydisperse particles were used to further optimize the matrix using parallel size distributions measured by an SMPS as a reference. Wang et al. (Submitteda) reported that the GMDs generated by the soot matrix agree with those reported by the SMPS within $\pm 20\%$ for 9.5–400-nm mono-disperse diesel engine exhaust particles. Similar improvements to the default matrix were made, and are now included in the compact matrix (Wang et al. Submittedb), but this matrix is not evaluated in this study because it was intended for compact rather than fractal vehicle-emitted particles.

This study further evaluates the performance of the new TSI soot matrix relative to the existing default matrix and reference size distributions measured by an SMPS over a variety of vehicle and engine-emitted polydisperse particles during steady-state conditions. Emission sources were a diesel generator, a light-duty gasoline direct injection (GDI) vehicle, a conventional light-duty gasoline port fuel injection (PFI)

vehicle, and a light-duty diesel (LDD) vehicle equipped with a diesel particulate filter (DPF). This selection of emission sources provides a broad spectrum of vehicle particulate from gasoline and diesel sources without wall-flow particulate after-treatment ($D_m = 2.2$ – 2.7), as well as particulate downstream of a DPF ($D_m = 2.3$ – 3.0) as discussed by Quiros et al. (2015a) to challenge the new soot matrix. This study evaluates the performance of the EEPS soot matrix using total particle number concentration, suspended particle mass determined by the IPSP method, and lognormal fitting statistics to either a unimodal or bimodal distribution (geometric mean diameter [GMD], geometric standard deviation [GSD], and area under the curve). We discuss the applicability of fast-sizing instruments, such as the EEPS, for providing “universal” accuracy when measuring particulate emissions from vehicle exhaust.

2. EXPERIMENTAL

2.1. Instruments: SMPS and EEPS

Size distributions were measured by an SMPS (Models 3936L76 and 3936L88) and an EEPS (Model 3090, firmware version 3.11), both manufactured by TSI Inc. Briefly, the SMPS measures particles that are first charged to a Fuchs charge distribution with a ^{85}Kr charger (Fuchs 1963; Wiedensohler 1988). The polydisperse particles are then separated in a Differential Mobility Analyzer (DMA) according to their electrical mobility. At each specific voltage, only particles with a specific electrical mobility are selected and counted by a downstream butanol- or water-based ultrafine condensation particle counter (CPC; TSI Model 3776 or 3788, respectively, cut-off size ~ 2.5 nm). The SMPS was operated with an inlet impactor with a cut-off aerodynamic diameter (d_{50}) of 620 nm. Due to the lower effective density of soot for large sizes, the impactor is likely not to be effective in term of multiple charge correction, but it may still protect the DMA from contamination by larger particles released from the walls of the sampling system or exhaust manifold. The SMPS was configured with aerosol and sheath flows equal to 1.45 and 7 L/min, respectively, a 2-min sampling resolution (up scan 90 s, down scan 30 s), and therefore the measured size distribution from 8.7 to 378.6 nm over 105 size bins. The data were analyzed with the TSI Aerosol Instrument Manager, version 8.0.0, and both diffusion loss and multiple charge corrections were used.

The EEPS charges particles efficiently using a unipolar corona charger. The charged particles are classified by electrical mobility, and then detected using multiple electrometers. One of the main differences between SMPS and EEPS is the particle charging mechanism. The SMPS uses a bipolar diffusion charger, while the EEPS uses a unipolar corona charger. As a result, the charging efficiencies for agglomerates are different. The EEPS is operated at 10 L/min for sample air, and 40 L/min for sheath air, and can measure particle sizes from

5.6 to 560 nm in a total of 32 size bins. This EEPS was operated with an inlet cyclone having a cut-off diameter of 1 μm , a 1-Hz data collection rate, and software version 3.2.5.0. Using this latest release of the TSI EEPS software, size distributions were exported using both default and soot matrices under the user-selectable menu option. The size distributions generated by the two matrices from the same raw instrument record were used for comparison with SMPS distributions in this study.

2.2. Test Vehicle, Fuel, and Matrix

Three light-duty passenger vehicles, including one GDI, one diesel vehicle, and one conventional gasoline PFI, and a diesel generator were used to generate particles and evaluate the PSD measurements. The GDI vehicle was a 2012 Mazda 3, which is certified to California PZEV II standards with a 2.0-L, 4-cylinder, wall-guided GDI engine and a three-way catalyst (TWC). The initial mileage was 19,155 miles. The diesel vehicle was a MY 2009 Volkswagen Jetta, equipped with a 2.0-L, 4-cylinder turbo-charged diesel engine, a DPF and a lean NO_x trap (LNT) system. The Jetta had an initial mileage of 114,331 miles and was certified to meet California ULEV II emissions standards. The PFI vehicle was a MY 2012 Chevrolet Malibu, which was certified to California ULEV II emission standards using a TWC among other controls, and had an initial mileage of 26,700 miles. The diesel generator was a Pramac 3.6-kW generator, E3750 MYHDI, Yanmar Engine that was not equipped with a DPF.

All the vehicles were tested with in-use California fuel purchased from a local fuel station, except the PFI vehicle was tested with Phase II certification fuel. The diesel generator was operated with commercial diesel fuel (ultralow sulfur diesel (ULSD), <15-ppm sulfur content) as well as a bio-fuel (fatty

acid methyl ester fuel B-100), which was a 100% biodiesel with 0.6-ppm sulfur content.

2.3. Laboratory Setup

All measurements except those on the PFI vehicle were made at the Vehicle Emissions Research Laboratory (VERL) of the Bourns College of Engineering-Center for Emissions Research and Technology (CE-CERT) at the University of California at Riverside (UCR). The testing cell in CE-CERT is equipped with a Burke E. Porter 48-inch single-roll electric dynamometer for LDVs. A schematic of the laboratory setup is shown in Figure S1 in the online supplementary information (SI). The CVS flow rate was set between 230 and 494 standard cubic feet per minute (CFM) (6.5–14 m^3/min) for LDVs, and to 1095 CFM (31 m^3/min) for diesel generator (Table 1). The CVS dilution air was HEPA-filtered. For diesel generator emissions, a mini-dilution tunnel (ISO-8178-1; Jayaram et al. 2011), which is equipped with a single venturi following ISO-8178-1, was used to provide a secondary dilution ratio of 9.5. The measurements on the PFI vehicle was conducted in the CARB Haagen-Smit Laboratory (HSL) located in El Monte, CA. Details regarding the HSL setup and configuration for the light-duty testing laboratory can be found in Hu et al. (2014) and Quiros et al. (2015a).

Table 1 lists the six testing configurations and specifications evaluated in this study. The passenger cars were tested at 30 or 60 mph with 0 to 4% simulated road grade, and the diesel generator was tested at a 1.34 bhp (≈ 1 kW) output. Vehicles were operated on a chassis dynamometer, and the diesel generator was used with a resistive load bank (Swift-E STD, Simplex Inc.) to ensure a consistent power output. The vehicles and generator were operated for 30 min prior to taking measurements to ensure thermal stability of engine

TABLE 1
Summary of testing conditions

Test ID	Vehicle/engine	Fuel	Operating condition	CVS flow rate (m^3/min)	2nd DF	No. of SMPS scans	Estimated mass-mobility exponent (D_m) ^{**}
Diesel-reg	Generator	ULSD	1.34 bhp	31	9.5	6	2.2
Diesel-bio	Generator	Biodiesel	1.34 bhp	31	9.5	6	2.2
GDI-30	Mazda 3	E10	30 mph at 0% grade	14	1	3	2.4
GDI-60	Mazda 3	E10	60 mph at 2% grade	14	1	3	2.3
PFI-25	Chevrolet Malibu	E10 Cert	25 mph* at 0.8% grade	6.5	1	37	2.7
TDI-60	VW Jetta	ULSD	60 mph at 4% grade	14	1	6	***

*Simulated transient operation, average speed 25 mph. Refer to Quiros et al. (2015a) for full description.

**Estimated mass-mobility scaling exponent based on the findings reported in Quiros et al. (2015a). Values equal to 3.0 indicate spherical particles; increasing fractal morphology is indicated by the decreasing values of D_m .

***The mass-mobility scaling exponent for particulates downstream of a wall-flow particulate filter is largely a function of operating condition, and is also likely specific to the age of the after-treatment system (Quiros et al. 2015a).

components and exhaust transfer lines. For each test, measurements were conducted for the duration required to make three complete SMPS scans (360 s). The PFI vehicle tested at HSL was warmed up for 15 min prior to beginning of measurement, and was operated continuously for 75 min while measurements were conducted. The PFI vehicle was operated under a simulated transient operation, where the speed of the vehicle was oscillated between approximately 23 and 27 mph once every 6 s. This condition was selected to evaluate the effect of transient operation on effective density in Quiros et al. (2015a), and on the performance of the EEPS inversion matrices in this article.

At VERL, the SMPS and EEPS sampled through the same line except for the last part of tubing connections. The SMPS sampled at a flow rate of 1.45 L/min from a copper tube with a length of 1.5 m. The EEPS sampled at a flow rate of 10 L/min from a copper tube with a length of 1.3 m. At HSL, the EEPS and SMPS directly sampled from a sampling manifold, drawing air from the CVS using conductive silicon tubing with a length of 1.25 m, and sample flow rates were 10 and 1.5 L/min respectively. The diffusional losses of particles onto sample tubing for both laboratories were calculated and corrected using the Gormley–Kennedy diffusion estimation (Gormley and Kennedy 1949). These losses were approximately 3% and 10% for 10-nm particles for the EEPS and SMPS sampling lines respectively, and were less than 0.1% for 400-nm particles measured by either instrument. The lower correction factor applied to the EEPS data can be attributed to the higher sample flow rate of the instrument. All data reported in this article have been corrected for any diffusional losses of particulate before entering the instrument.

3. DATA ANALYSIS

The IPSD method was initially defined by Liu et al. (2009), and more recently evaluated using emissions from LDVs by Li et al. (2014) and Quiros et al. (2015b), although the concept of using size distribution to estimate PM mass was discussed much earlier by Maricq and Xu (2004). Briefly, the IPSD method estimates total particle mass by integrating the fractional mass obtained by multiplying the particle effective density and volume concentration for each size bin from the measured PSD as follows:

$$M_{\text{IPSD}} = \sum_i \rho_{\text{eff},i} \left(\frac{\pi D_{p,i}^3}{6} \right) n_i, \quad [1]$$

where n_i and $D_{p,i}$ are the particle number concentration and particle mobility diameter, respectively, in a given size bin i , and $\rho_{\text{eff},i}$ is the effective density of the particle in size bin i . The effective density is dependent on particle composition and morphology (Park et al. 2003) and can be expressed as a

function of a mass-mobility scaling exponent (D_m) and constant A :

$$\rho_{\text{eff}} = \frac{6AD_p^{D_m-3}}{\pi} \quad (D_p \geq 55 \text{ nm}) \quad [2]$$

Using the power decay model, effective density is not well predicted for nucleation mode particles. Therefore, in this study, a constant density of hydrated sulfuric acid (1.46 g/cm³) was assumed for particle diameters smaller than 30 nm (Zheng et al. 2012). For all particles larger than 55 nm, Equation (2) was used to calculate the particle effective density using data from Maricq and Xu (2004) for GDI vehicles ($D_m = 2.2$, $A = 13.3$, D_p (units nm) and ρ_{eff} (units g/cm³)). For particles with D_p between 30 and 55 nm, the effective density calculated for particles with $D_p = 55$ nm (1.031 g/cm³) was applied, which fits with experimental data well shown in previous studies within this range (Maricq and Xu 2004; Quiros et al. 2015b).

Note that the estimates of suspended PM mass using ISPD used the same effective density functions, despite the known (or expected) differences in effective density among various emission sources. The only difference between matrices for the number and mass distributions is the measurement method (SMPS, EEPS default matrix, and EEPS soot matrix). In Section S1, Table S1 in the SI, we quantify the impact of changing the effective density function on final mass estimates. The impacts of changing effective density on final mass estimation are generally minimal. The estimated mass-mobility scaling exponents, which are used to model effective density as a function of size, are listed for each vehicle condition in Table 1. Technically these values are the exponents in the power-fit model used to relate mobility diameter with particle mass; in addition, these can be used to assess the morphology of a given particle. Values equal to 3.0 indicate a spherical particle, with increasing branched and fractal morphologies indicated by decreasing values of D_m . These exponents are used to compare the strengths and weaknesses of two EEPS inversion matrices for measuring PSD relative to reference SMPS distributions.

4. RESULTS AND DISCUSSION

Particle size distributions, total particle number concentrations, and total PM mass determined by the IPSD method (M_{IPSD}) from EEPS and SMPS are shown in Figures 1–5 and Table 2. The vertical error bars represent one standard deviation (SD) of the measurements either during three or six consecutive SMPS scans to compare average PSDs. These error bars reflect both measurement uncertainty and actual variations in vehicle emissions over the measurement period. For this reason, no vertical error bars are shown in Figure 4, which represents a notably longer and transient measurement period. To compare the SMPS and EEPS distributions only for the

regions of overlapping size ranges between 8.7 nm and 378.6 nm, the integrated number and mass emissions are reported within this range only. Particle size distributions were fit to lognormal distributions, and corresponding GMDs and GSDs for nucleation and accumulation modes are listed in Table 3. The lognormal distributions fit to SMPS distributions are shown in Figures 1–5 for each test condition.

4.1. Diesel Generator

4.1.1. Diesel Generator Operated with ULSD (Strong Unimodal Distribution)

Figure 1 shows size distributions reported when measuring emissions from the diesel generator using ULSD. Based on reference SMPS measurements, the distribution is a unimodal with a GMD of 52 nm. This GMD is consistent with previous studies (Harris and Maricq 2001; Zervas and Dorlhene 2006) and suggests that the majority of the particles are accumulation mode soot particles with a mass-mobility scaling exponent of approximately 2.2 (Mariq and Xu 2004; Olfert et al. 2007). We expect this condition to represent the relative performance

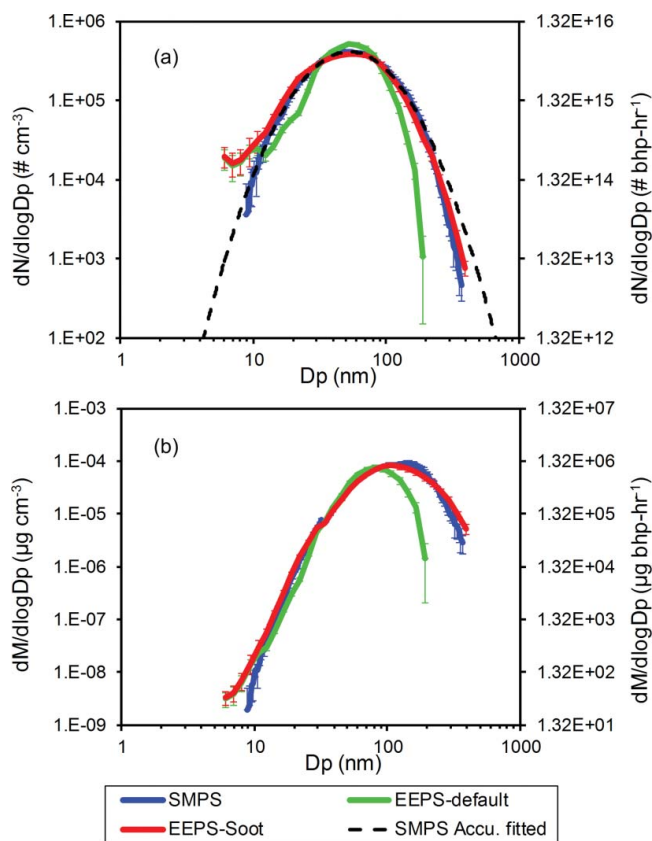


FIG. 1. (a) Number, and (b) mass distributions reported by SMPS and EEPS default and soot matrices for the diesel generator operating on ULSD. Dashed lines in panel (a) present lognormal-fitted size distribution of accumulation mode particles measured by SMPS. The equivalent work-based emission factors for number and mass are presented on the right y-axis.

of the size distribution methods when measuring diesel exhaust from engines operating on ULSD without DPF after-treatment. The particle number emission and particle mass emission rates determined by the IPSD method (M_{IPSD}) were $3.71 \pm 0.05 \times 10^{15}$ #/bhp-h (average \pm SD) and 672 ± 28 mg/bhp-h (Table 2) respectively based on reference SMPS measurements.

The size distributions measured by the EEPS with the default matrix showed a bimodal distribution with a small nucleation mode with a GMD of 12 nm, and an accumulation mode with a GMD of 54 nm (Figure 1a and Table 3). Although the accumulation mode GMD was similar to that of SMPS (52 nm), it is notable that the default matrix for the EEPS resulted in a much narrower size distribution (GSD = 1.55) compared with the size distribution measured by the SMPS (GSD = 1.87). The EEPS default matrix underestimated particle number in the 10.8 to 34-nm and 93.1 to 371.8-nm size bins, and overestimated particle number in the 34 to 93.1 nm size bins. Harris and Maricq (2001) used the SMPS to measure the size distribution of diesel soot emitted from both diesel engines and LDD vehicles equipped with oxidation catalysts. They reported that diesel soot size distributions were well described by a single signature lognormal curve with a GSD of ~ 1.7 nm for diesel vehicles, and ~ 1.8 nm for two sets of diesel engines. The GSDs measured in this study with the EEPS default matrix were significantly smaller because the default matrix was developed using near-spherical particles and does not correctly represent the charging and detection of soot particles in the EEPS as discussed by Wang et al. (Submitted a,b). In addition, the EEPS detected a small nucleation mode that was not observed by the SMPS. The cause of this peak is unclear, and was detected by the soot matrix as well.

The M_{IPSD} value estimated with the EEPS default matrix was 417 ± 37 mg/bhp-h, 38% lower than that estimated by the SMPS. This is explainable because the default matrix underestimates the emission rate of larger particles, and the particle mass is the 2.2 power of particle diameter (volume increases by a cubic power, but effective density decreases by a 0.8 power of mobility diameter). The particle number emission rate of PM estimated by the EEPS default matrix was $3.48 \pm 0.15 \times 10^{15}$ #/bhp-h, close to that estimated by the SMPS.

When the soot matrix was applied, the diesel exhaust PSDs showed a bimodal distribution with a nucleation and accumulation mode diameters of 10 nm and 52 nm respectively (Figure 1a and Table 3). Particle mass distribution was calculated using the IPSD method in Figure 1b. A notable improvement in the particle sizing was observed, especially in the large particle sizes ($> \sim 100$ nm). The GSD of the single lognormal fit was 1.90 nm, slightly larger but in close agreement to the GSD measured by the SMPS (1.87 nm). The response of the EEPS soot matrix for measuring particle number and mass for particles was slightly larger than the reference SMPS measurements for

TABLE 2
Particle number and mass emission rates (M_{IPSD}) determined by EEPS and SMPS*

	Particle number emission rate		
	SMPS	EEPS default	EEPS soot
Diesel-reg (#/bhp-h)	$3.71 \pm 0.05 \times 10^{15}$	$3.48 \pm 0.15 \times 10^{15}$	$3.69 \pm 0.12 \times 10^{15}$
Diesel-bio (#/bhp-h)	$3.08 \pm 0.18 \times 10^{15}$	$2.25 \pm 0.12 \times 10^{15}$	$2.73 \pm 0.18 \times 10^{15}$
GDI-30 (#/mile)	$3.18 \pm 0.26 \times 10^{11}$	$2.28 \pm 0.88 \times 10^{11}$	$3.46 \pm 1.32 \times 10^{11}$
GDI-60 (#/mile)	$1.40 \pm 0.18 \times 10^{12}$	$1.09 \pm 0.25 \times 10^{12}$	$1.37 \pm 0.30 \times 10^{12}$
PFI-25 (#/mile)	$3.08 \pm 1.81 \times 10^{12}$	$3.39 \pm 3.30 \times 10^{12}$	$3.89 \pm 3.73 \times 10^{12}$
TDI-60 (#/mile)	$3.87 \pm 0.53 \times 10^{14}$	$2.03 \pm 0.24 \times 10^{12}$	$3.01 \pm 0.33 \times 10^{12}$
	Particle mass emission rate (M_{IPSD})		
	SMPS	EEPS default	EEPS soot
Diesel-reg (mg/bhp-h)	672 ± 28	417 ± 37	630 ± 62
Diesel-bio (mg/bhp-h)	236 ± 6	162 ± 10	240 ± 17
GDI-30 (mg/mile)	0.018 ± 0.006	0.012 ± 0.004	0.016 ± 0.006
GDI-60 (mg/mile)	0.15 ± 0.03	0.10 ± 0.02	0.15 ± 0.03
PFI-25 (mg/mile)	0.46 ± 0.32	0.34 ± 0.38	0.52 ± 0.56
TDI-60 (mg/mile)	1.17 ± 0.14	0.12 ± 0.01	0.17 ± 0.01

*Total particle number and PM mass emission rates account for CVS flow rates and secondary dilution factors.

particles between ~200 nm and 400 nm. However, the overall estimated M_{IPSD} was 630 ± 62 mg/bhp-h, which is 6% lower than the SMPS measurement (672 ± 28 mg/bhp-h). Overall, an excellent agreement is shown between the

SMPS and EEPS soot matrix, indicating an improvement in EEPS for measuring particle number and mass emissions for traditional diesel exhaust with a dominant accumulation mode.

TABLE 3
Parameters for bi-modal fit of each steady state test

Test ID	Instrument/matrices	Nucleation mode			Accumulation mode		
		Fraction (%) ¹	GMD (nm) ²	GSD ³	Fraction (%)	GMD (nm)	GSD
Diesel-reg	SMPS	0	—	—	100	52	1.87
	EEPS default	5	12	1.80	95	54	1.55
	EEPS soot	3	10	1.80	97	52	1.90
Diesel-bio	SMPS	12	11	1.30	88	43	1.71
	EEPS default	12	11	1.31	88	44	1.53
	EEPS soot	13	11	1.28	87	41	1.77
GDI-30	SMPS	82.4	8	1.59	17.6	52	1.97
	EEPS default	71.1	8	1.48	28.9	37	1.84
	EEPS soot	58.6	9	1.33	41.4	24	2.42
GDI-60	SMPS	54	10	1.80	46	37	2.50
	EEPS default	34	11	1.44	66	52	1.73
	EEPS soot	30	11	1.29	70	37	2.50
PFI-25	SMPS	23.1	19	1.42	76.9	54	1.85
	EEPS default	22.7	13	1.53	97.3	52	1.63
	EEPS soot	32.5	15	1.61	67.5	51	1.92
TDI-60	SMPS	99.99	12	1.40	0.01	64	1.71
	EEPS default	89	6	1.57	11	61	1.50
	EEPS soot	89	8	1.43	11	66	1.60

¹Number fraction of particles in this mode.

²Geometric mean diameter (GMD).

³Geometric standard deviation (GSD).

4.1.2. Diesel Generator with Biodiesel (Weak Bimodal Distribution)

Figure 2 compares PSDs measured by the EEPS default and soot matrices and SMPS for the diesel generator operating on 100% biodiesel. All measured distributions exhibit a bimodal pattern, with a stronger accumulation mode and a weaker nucleation mode. Based on SMPS distributions, the particle number emission rate estimated was $3.08 \pm 0.18 \times 10^{15}$ #/bhp-h, which was 17% lower than when operating on ULSD as discussed in the previous section. However, M_{IPSD} decreased by 65% (from 672 ± 28 to 236 ± 6 mg/bhp-h) when the biodiesel was used due to decrease in accumulation mode particles. Interestingly, a nucleation mode with a GMD of ~ 10 nm was detected, which was not observed with ULSD. Given the extremely low sulfur content (0.6 ppm) of the biodiesel, the nucleation mode particles likely originated from lube oil. Because the same lube oil was used for regular diesel and biodiesel tests, it is possible that the reduced accumulation

mode particles with biodiesel resulted in greater condensational growth from gaseous hydrocarbons during dilution.

As shown in Figure 2a, PSDs reported by the EEPS matrices were also bimodal, with nucleation and accumulation mode GMDs of ~ 11 nm and ~ 44 nm, respectively, for both matrices, and close to those reported by SMPS. The agreement of the EEPS default and soot matrices for reporting GMD is interesting because the default matrix was calibrated by near-spherical laboratory-generated particles for all size ranges, whereas the soot matrix was calibrated using engine-generated particles for both nucleation and accumulation modes (Wang et al. Submitteda). These results indicate that nucleation mode particles emitted from a generator operating on low sulfur content bio-fuel possess similar properties as laboratory- and engine-generated calibration materials, and generally exhibit good size-based agreement. Also, the result indicates that particle charging characteristics are not much different between near-spherical and aggregates at small sizes more specifically of around 44 nm.

Figure 2a shows that the default matrix generally underestimated the particle number for all size bins, including nucleation mode and larger accumulation mode particles. The total particle number emission rate given by the EEPS default matrix was $2.25 \pm 0.12 \times 10^{15}$ #/bhp-h, 27% lower than that estimated by SMPS. Meanwhile, the EEPS default matrix underestimated the GSD of accumulation mode compared with SMPS (1.53 vs. 1.71). As shown by mass distributions in Figure 2b, the estimated M_{IPSD} for the EEPS default matrix was 162 ± 10 mg/bhp-h, 31% lower than that estimated by SMPS (236 ± 6 mg/bhp-h).

Figure 2a shows that the EEPS soot matrix substantially improved agreement between the EEPS and SMPS size distributions for all size ranges, but some discrepancies still exist. As shown in Table 2, the particle number and mass emission rate given by the EEPS soot matrix was $2.73 \pm 0.18 \times 10^{15}$ #/bhp-h and 240 ± 17 mg/bhp-h, which agreed within 11% and 2%, respectively, with those estimated by the SMPS ($3.08 \pm 0.18 \times 10^{15}$ #/bhp-h and 236 ± 6 mg/bhp-h respectively). Wang et al. (Submitteda,b) found that EEPS may underestimate particle concentrations < 10 nm, but could not get high enough signal-to-noise ratio to calibrate EEPS in that size range. To address the issue, they increased the gain of the lowest channels (5.6 and 7.5 nm) by $\sim 10\%$ to account for the part of underestimation while not generating artifacts due to electrometer noise. The soot matrix also reported a smooth continuous distribution between ~ 100 nm and 300 nm that the default matrix did not report above the detection limit of the instrument. In this range, although the soot matrix achieved better agreement than the default matrix, it over-predicted the number and especially the mass distributions relative to SMPS reference measurements. It is possible that the morphology of the accumulation mode particles may have differed compared with the emissions generated by the engine used for EEPS calibration, and thereby resulted in a slightly greater response. A

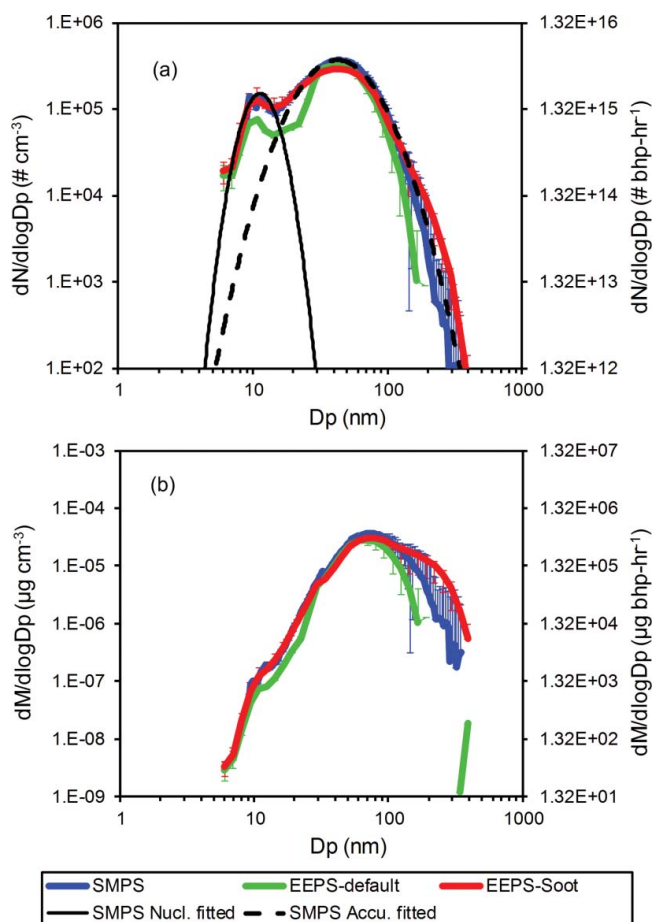


FIG. 2. (a) Number, and (b) mass distributions reported by SMPS and EEPS default and soot matrices for the diesel generator operating on biodiesel. Dashed lines in panel (a) present lognormal-fitted size distribution of accumulation mode particles measured by SMPS. The equivalent work-based emission factors for number and mass are presented on the right y-axis.

direct measurement of effective density or mass-mobility scaling exponent could provide some indication as to whether particle morphology played a role in the observed over-prediction of accumulation mode particles when characterizing emissions from a diesel generator fueled by biodiesel.

4.2. GDI Vehicle (Balanced Bimodal Distribution with a Lower Mass-Mobility Scaling Exponent)

Figure 3 compares PSDs measured by EEPS and SMPS for a GDI vehicle (the Mazda 3) operated at 60 mph and a 2% simulated road grade. The SMPS reported a bimodal size distribution with GMDs of 10 nm and 37 nm for nucleation and accumulation modes, respectively. The PSD under the test condition for this vehicle gave a strongly overlapping bimodal distribution; the nucleation mode contributed 54% to the total particle number, a substantial increase than the small

nucleation mode observed when characterizing emissions from the diesel generator operating on bio-fuel. Although not measured directly, we estimate the mass-mobility scaling exponent of PSD to be approximately 2.3 based on the steady-state measurements of modern GDI vehicles conducted by Quiros et al. (2015a).

Similar to the patterns observed when measuring emissions from the diesel generator, the EEPS default matrix showed substantial disagreement with size distributions reported by SMPS when measuring light-duty GDI emissions. As shown in Figure 3a, the EEPS default matrix reported narrower accumulation mode distributions than the SMPS (GSD = 1.73 nm vs. 2.50 nm), which resulted in underestimating the number concentration of particles larger than 100 nm by one to several orders of magnitude. Over both nucleation and accumulation modes, total particle number emissions reported by the EEPS default matrix were $1.09 \pm 0.25 \times 10^{12}$ #/mile (22% lower than the SMPS), and mass emissions were 0.10 ± 0.02 mg/mile (33% lower than the SMPS). This observation of the historical TSI EEPS default matrix is a likely key contributor to the observed 34% underestimation of M_{IPSD} relative to gravimetric filters when we evaluated the IPSD method using the transient FTP cycle (Li et al. 2014).

The EEPS soot matrix exhibited substantially stronger agreement with reference SMPS distributions than the EEPS default matrix for light-duty GDI emissions. Better agreement is observed with nucleation mode particles between 10 nm and 20 nm due to the increased gain for channels in that size range as explained previously. The nucleation mode GSD of SMPS distribution (1.80) was notably broader than either EEPS matrix (1.29 and 1.44); however, the accumulation mode GSD for the SMPS and EEPS soot matrix are identical (2.50) and notably larger than the EEPS default matrix (1.73). Overall, total particle number and mass (M_{IPSD}) emission rates were estimated to be $1.37 \pm 0.30 \times 10^{12}$ #/mile and 0.15 ± 0.03 mg/mile, respectively, agreeing with those measured by SMPS within 2% ($1.40 \pm 0.18 \times 10^{12}$ #/mile and 0.15 ± 0.03 mg/mile respectively). Figure 3b illustrates the mass distributions, and shows a good agreement between the EEPS soot matrix and the SMPS measurements. These findings suggest that the new EEPS soot matrix appears to accurately characterize both number and mass distributions in both nucleation and accumulation modes when challenged by light-duty GDI vehicle particulate emissions.

A comparison of the EEPS with the default matrix and soot matrix was also conducted at a lower speed (30 mph) and 0% grade to challenge the EEPS with different exhaust PSDs and lower concentrations from the GDI vehicle. The result also shows that with the default matrix, the EEPS tended to underestimate particle number and mass emission rate, in comparison with the measurement of SMPS, while the soot matrix improved the agreements between EEPS and SMPS with both particle number and mass emission rate. More detailed discussion is provided in Section S2 and Figure S2 in the SI.

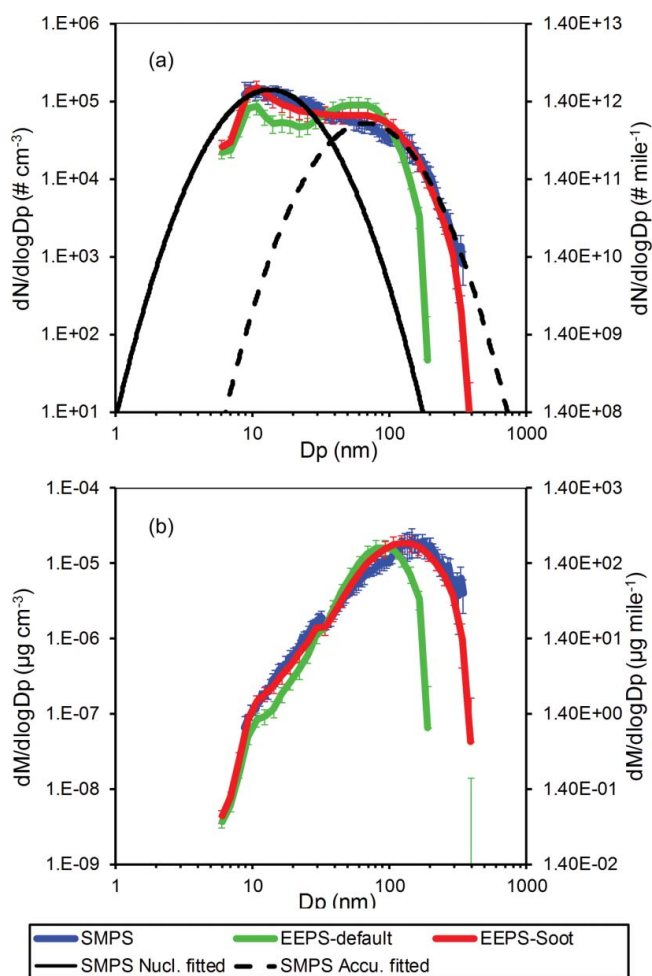


FIG. 3. (a) Number, and (b) mass distributions reported by SMPS and EEPS default and soot matrices for the GDI vehicle operating at 60 mph and 2% road grade. Dashed lines in panel (a) present lognormal-fitted size distribution of nucleation and accumulation mode particles measured by SMPS. The equivalent distance-based emission factors for number and mass are presented on the right y-axis.

4.3. PFI Vehicle (Balanced Bimodal Distribution with a Higher Mass-Mobility Scaling Exponent)

Figure 4 compares PSDs measured by EEPS and SMPS for a PFI vehicle (Chevrolet Malibu) operated at 25 mph and a 0.8% simulated road grade at the ARB light-duty HSL. The distribution was bimodal with GMDs of 19 and 54 nm for nucleation and accumulation modes, respectively. The accumulation mode contributed 76.9% of the total particle number, with the rest contributed by nucleation mode particles. The testing was conducted by Quiros et al. (2015a), and the measured mass-mobility scaling exponent of the emissions during this test was 2.7. Compared with the emissions generally reported by GDI vehicles, the mass of particulates from PFI vehicles scale more rapidly with increasing diameter, indicating more compact geometries for larger particles and more filling of the void space of soot particles.

The relative differences between SMPS, EEPS default matrix, and EEPS soot matrix distributions were similar to those observed for the diesel generator and light-duty GDI

vehicle, with a couple of important exceptions. In contrast to the vehicle emissions with lower mass-mobility scaling exponent, total particle number emission rates measured with the EEPS default matrix was $3.39 \pm 3.30 \times 10^{12}$ #/mile, 10% higher than that estimated by SMPS ($3.08 \pm 1.81 \times 10^{12}$ #/mile). In addition, the EEPS default matrix gave a similar GMD for accumulation mode particles compared with SMPS (52 nm vs. 54 nm). Similar to the trends observed in Figures 1–3, the GSD of accumulation mode particles was much narrower for the EEPS default matrix than the SMPS (GSD = 1.63 vs. 1.85, Table 3). Similarly, this resulted in lower overall mass estimates (M_{IPSD}) for the EEPS default matrix reporting a 26% lower mass estimate (0.34 ± 0.38 mg/mile) compared with the SMPS (0.46 ± 0.32 mg/mile). When the EEPS soot matrix was applied, the agreement in accumulation mode particle sizing given by the two instruments was improved when characterizing particle mass emissions, but not necessarily particle number emissions that are typically influenced by nucleation mode particles. The broadening of

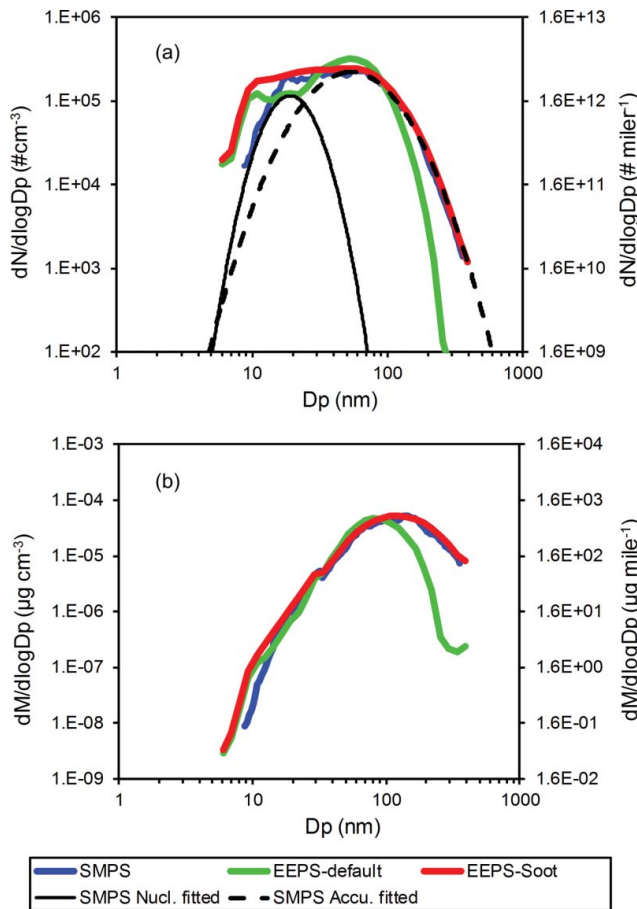


FIG. 4. (a) Number, and (b) mass distributions reported by SMPS and EEPS default and soot matrices for the PFI vehicle operating at 25 mph and 0.8% road grade under a simulated transient operation mode. Dashed lines in panel (a) present lognormal-fitted size distribution of nucleation and accumulation mode particles measured by SMPS. The equivalent distance-based emission factors for number and mass are presented on the right y-axis.

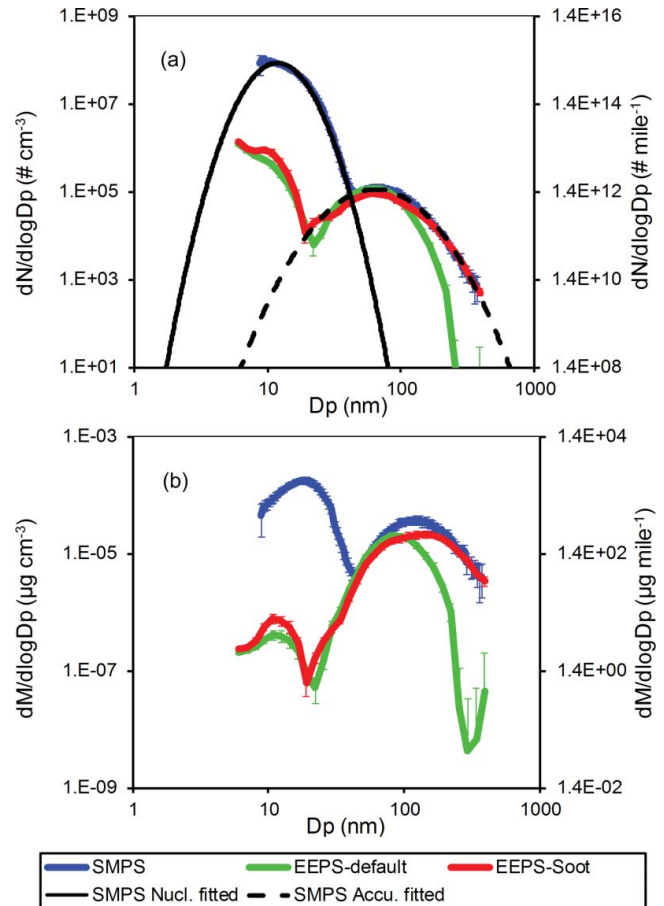


FIG. 5. (a) Number, and (b) mass distributions reported by SMPS and EEPS default and soot matrices for the TDI vehicle operating at 60 mph and 4% road grade. Dashed lines in panel (a) present lognormal-fitted size distribution of nucleation and accumulation mode particles measured by SMPS. The equivalent distance-based emission factors for number and mass are presented on the right y-axis.

the accumulation mode GSD resulted in better mass agreement between EEPS soot matrix (0.52 ± 0.56 mg/mile) and reference SMPS measurements (0.46 ± 0.32 mg/mile). Given the EEPS soot matrix was developed based on emissions from an off-road diesel engine, likely with a much lower mass-mobility scaling exponent, it is interesting to observe good agreement for mass distributions, especially for larger particle sizes as observed in Figure 4. Unipolar diffusion charging of particles depends on particle morphology. Jung and Kittelson (2005) found diesel soot assumedly with $D_m = \sim 2.3$ obtains 15 to 17% more charges than singlets with $D_m = \sim 3$. It is interesting that no difference was observed when the soot matrix was used for aerosol with $D_m = \sim 2.7$ while the matrix was developed using aerosol with $D_m = \sim 2.3$. Further investigation is necessary in this aspect.

However, the EEPS soot matrix resulted in a larger deviation when measuring total particle number emissions relative to the SMPS distribution. The EEPS default matrix overestimated the total particle number emissions relative to SMPS distributions by 10%, and the new EEPS soot matrix overestimated total particle number by 26%. As shown in Figure 4a, the deconvolution of the total size distribution into “nucleation” and “accumulation” modes is not entirely clear, where differences in the nucleation mode between the three size distributions were reported.

4.4. Turbo-Charged Direct Injection LDD Vehicle with a DPF (Strong Bi-Modal Distribution)

Figure 5 compares PSDs for the turbo-charged direct injection (TDI) operated at 60 mph and 4% road grade (test ID: TDI-60 in Table 1). This vehicle was field-aged near the end of the regulatory useful life period, and the originally equipped DPF likely accumulated sulfur and other elements originating from lube oil or diesel over this period that could affect particle mass emissions. All three size distributions exhibited a bimodal trend, with a dominant nucleation mode centered at ~ 10 nm as measured by SMPS.

Similar size distributions were observed with heavy-duty diesel vehicles equipped with DPFs, where Herner et al. (2011) demonstrated that nucleation mode emissions are catalyst temperature-dependent, and comprise up to 62% sulfate by reconstructed mass. As a result of high load, the catalyst temperature for this condition was 452°C , which is sufficient to promote oxidation of SO_2 to SO_3 , which quickly reacts with water vapor to form H_2SO_4 . Therefore, the nucleation mode observed from the TDI vehicle was likely hydrated sulfate with possible condensed hydrocarbons formed during dilution rather than solid particles formed during combustion that are typically removed by DPF (De Filippo and Maricq 2008). It is important to note that the elevated temperature was the result of high load operation (60 mph, 4% simulated road grade), and the resulting emissions are not likely observed during most certification cycles such as the FTP or

Supplemental FTP (US06) that only momentarily reach these power outputs.

Figure 5a illustrates that the EEPS soot matrix provided partial improvement upon the default matrix when characterizing particle number, and little improvement when characterizing particle mass, relative to SMPS distributions. The default and soot matrices significantly underestimated total particle number emission rate by 48% and 21%, relative to SMPS, respectively. Nevertheless, the accumulation mode of the EEPS data inverted by the new soot matrix exhibited substantial broadening, and agreed more closely with SMPS than that by the default matrix (Figure 5a). However, since the nucleation mode dominated the distribution and accounted for $\sim 80\%$ of the particle mass emissions, the EEPS highly underestimated total particle mass emissions.

The discrepancy when measuring nucleation mode particle number emissions possibly came from the fact that nucleation mode particles have grown to different concentrations and sizes at the point the particles were measured by SMPS and EEPS. The EEPS had a higher sample flow rate, and therefore shorter transit time through the sampling line (0.1 s) than the SMPS (0.8 s), and therefore less time for growth (Wei et al. 2001). We believe the discrepancy is due to sampling conditions as many studies have reports that bipolar and unipolar charging showed negligible difference for sphere particles (Jiang et al. 2011). Sampling of nucleation mode particles is a challenge and there is continuous effort seeking for optimal sampling conditions (Kittleson et al. 2002). One suggestion is to use a secondary dilution to equilibrate nucleation mode particles; however, the selection of dilution ratio requires empirical practice. Humidity and temperature of dilution air/sample should also be considered. The sample transit time should be another parameter to be considered (Vouitsis et al. 2008). Future work should be conducted for further investigation.

5. CONCLUSIONS

In this study, size distributions reported by the TSI EEPS using the default matrix and a new kernel matrix, the soot matrix, were compared with measurements with an SMPS over steady-state conditions. To represent different engine technologies with expected mass-mobility scaling exponents between 2.2 and 2.7, tests were conducted using a GDI vehicle, a conventional gasoline PFI vehicle, one LDD vehicle equipped with a DPF, and a diesel generator. Over all the conditions evaluated in Figures 1–5, the EEPS soot matrix greatly improved the agreement with SMPS for most cases, particularly for number and mass distribution of particles larger than 100 nm. For mass concentrations, the soot matrix agreed with SMPS within 13%, and for number concentrations the soot matrix agreed within 26% when excluding the TDI test for number concentration comparison.

As pointed out by Wang et al. (Submitted a,b), the EEPS instrument matrices are ill-conditioned, i.e., particles of the

same mobility diameter can be detected by several electrometers. The overlapping of matrix columns enables size distributions with a range of width to be able to fit to the EEPS electrometer data. The mathematical regularization in the inversion process further favors the smoothest solution, resulting in a broader distribution. Therefore, the EEPS resolution is less than that of the SMPS resolution, and generally performs better with smooth and broad unimodal distributions (Figures 1 and 2), but may have challenges in retrieving narrow distributions or distributions with fine features, such as bimodal or non-typical size distributions that may appear more mono-disperse in nature (Figure 4).

Overall, the EEPS soot matrix is a broad and strong improvement upon the default matrix, and appears to reasonably agree with the SMPS reference measurements for typical size distributions emitted from modern vehicle exhaust. Atypical size distributions measured from the TDI vehicle equipped with DPF after-treatment did not agree as well, and the flexibility of the TSI EEPS running the soot matrix should be further explored for a wider range of size distributions. Next, the “universality” of the EEPS soot matrix for vehicle-emitted particulates could further be tested over transient test cycles, and verified against other reference measurements such as the gravimetric method for mass determination.

ACKNOWLEDGMENTS

Heejung S. Jung and Xiaoliang Wang thank TSI for technical support and permission on the use of the new soot matrix before its official release. The authors thank Kurt Bumiller for his contribution in conducting the emissions testing for this program.

FUNDING

This program was supported by the California Air Resources Board under contract 11-548.

SUPPLEMENTAL MATERIAL

Supplemental data contain Section S1: Variations in particle mass emissions due to uncertainties in particle densities for nucleation mode, and Section S2: Size distribution of SMPS and EEPS with Mazda 3 GDI at 30 mph. Supplemental data for this article can be accessed on the publisher’s website.

REFERENCES

Asbach, C., Kaminski, H., Fissan, H., Monz, C., Dahmann, D., Mulhopt, S., Paur, H. R., Kiesling, H. J., Herrmann, F., Voetz, M., and Kuhlbusch, T. A. J. (2009). Comparison of Four Mobility Particle Sizers With Different Time Resolution for Stationary Exposure Measurements. *J. Nanopart. Res.*, 11:1593–1609.

Biskos, G., Reavell K., and Collings N. (2005). Description and Theoretical Analysis of a Differential Mobility Spectrometer. *Aerosol Sci. Technol.*, 39:527–541.

CARB. (2012). *LEV III PM, Technical Support Document – Development of Particulate Matter Mass Standards for Future Light-Duty Vehicles. Staff Report.* California Air Resources Board, CA.

Chang, J.S. (1981). Theory of Diffusion Charging of Arbitrarily Shaped Conductive Aerosol Particles by Unipolar Ions. *J. Aerosol Sci.*, 12:19–26.

De Filippo, A., and Maricq, M. M. (2008). Diesel Nucleation Mode Particles: Semi-volatile or Solid? *Environ. Sci. Technol.*, 42:7957–7962.

Donaldson, K., Li, X. Y., and Macnee, W. (1998). Ultrafine (Nanometre) Particle-Mediated Lung Injury. *J. Aerosol Sci.*, 29:553–560.

Fuchs, N. A. (1963). On the Stationary Charge Distribution on Aerosol Particles in a Bipolar Ionic Atmosphere. *Geofisica Pura Applicata*, 56:185–193.

Gormley, P. G., and Kennedy, M. (1949). Diffusion from a Stream Flowing Through a Cylindrical Tube. *Proc. Royal Irish Acad.*, 52(A)163–169.

Harris, S. J., and Maricq, M. M. (2001). Signature Size Distributions for Diesel and Gasoline Engine Exhaust Particulate Matter. *J. Aerosol Sci.*, 32:749–764.

Herner, J. D., Hu, S. H., Robertson, W. H., Huai, T., Chang, M. C. O., Rieger, P., and Ayala, A. (2011). Effect of Advanced Aftertreatment for PM and NOx Reduction on Heavy-Duty Diesel Engine Ultrafine Particle Emissions. *Environ. Sci. Technol.*, 45:2413–2419.

Hu, S., Zhang, S., Sardar, S., Chen, S., DzHEMA, I., Huang, S.-M., Quiros, D., Sun, H., Laroo, C., Sanchez, L. J., Watson, J., Chang, O. M.-C., Huai, T., and Ayala (2014). An Evaluation of Gravimetric Method to Measure Light-Duty Vehicle Particulate Matter Emissions at Levels Below One Milligram per Mile (1 mg/mile) *SAE Technical Paper* 2014-01-1571.

ISO-8178-1. (2006). Reciprocating Internal Combustion Engines – Exhaust Emission Measurement – Part 1: Test-Bed Measurement of Gaseous and Particulate Exhaust Emissions. Available at: http://www.iso.org/iso/catalogue_detail.htm?csnumber=42714 (accessed 9 September 2015).

Jayaram, V., Agrawal, H., Welch, W. A., Miller, J. W., and Cocker, D. R. (2011). Real-Time Gaseous, PM and Ultrafine Particle Emissions from a Modern Marine Engine Operating on Biodiesel. *Environ. Sci. Technol.*, 45:2286–2292.

Jeong, C. H., and Evans, G. J. (2009). Inter-Comparison of a Fast Mobility Particle Sizer and a Scanning Mobility Particle Sizer Incorporating an Ultrafine Water-Based Condensation Particle Counter. *Aerosol Sci. Technol.*, 43:364–373.

Jiang, J., Chen, M., Kuang, C., Attoui, M., and McMurry, P.H. (2011). Electrical Mobility Spectrometer Using a Diethylene Glycol Condensation Particle Counter for Measurement of Aerosol Size Distributions Down to 1 nm. *Aerosol Sci. Technol.*, 45:510–521.

Johnson, T., Caldwell, R., Pocher, A., Mirme, A., and Kittelson, D. B. (2004). An New Electrical Mobility Particle Sizer Spectrometer for Engine Exhaust Particle Measurements. *SAE Technical Paper* 2004-01-1341. Society of Automotive Engineers.

Johnson, T., Kittelson, D. B., Mirme, A., Caldwell, R., and Philips, A. (2003). An Engine Exhaust Particle Sizer Spectrometer for Transient Emission Particle Measurements. *9th Diesel Engine Emissions Reduction (DEER) Workshop 2003*, Newport, RI.

Jung H.J., and Kittelson D.B. (2005). Characterization of Aerosol Surface Instruments in Transition Regime. *Aerosol Sci. Technol.*, 39:902–911

Kaminski, H., Kuhlbusch, T. A. J., Rath, S., Gotz, U., Sprenger, M., Wels, D., Polloczek, J., Bachmann, V., Dziurawitz, N., Kiesling, H. J., Schwiigelshohn, A., Monz, C., Dahmann, D., and Asbach, C. (2013). Comparability of Mobility Particle Sizers and Diffusion Chargers. *J. Aerosol Sci.*, 57:156–178.

Khalek, I., Bougher, T., and Jetter, J. (2010). Particle Emissions from a 2009 Gasoline Diesel Injection Engine Using Different Commercially Available Fuels. *SAE Technical Paper* 2010-01-2117. Society of Automotive Engineers.

- Kinney, P. D., and Pui, D. Y. (1991). Use of the Electrostatic Classification Method to 0.1 μm SRM Particles-A Feasibility Study. *J. Res. Natl. Inst. Stand. Technol.*, 96:147-176.
- Kittelson, D. B., Watts, W. F., and Johnson, J. P. (2002). *Diesel Aerosol Sampling Methodology*. CRC E-43 Final Report, Coordinating Research Council, Alpharetta, GA.
- Lehmann U., Niemela V., and Mohr M. (2004). New Method for Time-Resolved Diesel Engine Exhaust Particle Mass Measurement. *Environ. Sci. Technol.*, 38:5704-5711.
- Li, Y., Xue, J., Johnson, J. P., Durbin, T. D., Villeta, M., Pham, L., Hosseini, S., Zheng, Z., Short, D., Karavalais, G., Awuku, A., Jung, H. J., Wang, X. L., Quiros, D., Hu, S. H., Huai, T., and Ayala, A. (2014). Determination of Suspended Exhaust PM Mass for Light-Duty Vehicles. *SAE Technical Paper* 2014-01-1594. Society of Automotive Engineers.
- Liu, Z. G., Thururow, E. M., Caldow, R., and Johnso, T. R. (2005). Transient Performance of Diesel Particulate Filters as Measured by an Engine Exhaust Particle Size Spectrometer. *SAE Technical Paper*, 2005-01-0185.
- Liu, Z. G., Vasys, V. N., Dettmann, M. E., Schauer, J. J., Kittelson, D. B., and Swanson, J. (2009). Comparison of Strategies for the Measurement of Mass Emissions from Diesel Engines Emitting Ultra-Low Levels of Particulate Matter. *Aerosol Sci. Technol.*, 42:1142-1152.
- Mamakos A., Ntziachristos L., and Samaras Z. (2006). Evaluation of the Dekati Mass Monitor for the Measurement of Exhaust Particle Mass Emissions. *Environ. Sci. Technol.*, 40:4739-4745.
- Maricq, M. M., and Xu N. (2004). The Effective Density and Fractal Dimension of Soot Particles from Premixed Flames and Motor Vehicle Exhaust. *J. Aerosol Sci.*, 35:1251-1274.
- Maricq, M. M., Xu N., and Chase R. E. (2006). Measuring Particulate Mass Emissions with the Electrical Low Pressure Impactor. *Aerosol Sci. Technol.*, 40:68-79.
- Mirme, A. (1994). *Electric Aerosol Spectrometry*. Doctoral thesis, Tartu University, Tartu, Estonia.
- Mulholland, G. W., Donnelly, M. K., Hagwood, C. R., Kukuck, S. R., Hackley, V. A., and Pui, D. Y. H. (2006). Measurement of 100-nm and 60-nm Particle Standards by Differential Mobility Analysis. *J. Res. Nat. Inst. Stand. Technol.*, 111:257-312.
- Oberdorster, G., Sharp, Z., Atudorei, V., Elder, A., Gelein, R., Kreyling, W., and Cox, C. (2004). Translocation of Inhaled Ultrafine Particles to the Brain. *Inhalation Toxicol.*, 16:437-445.
- Oh, H., Park, H., and Kim, S. (2004). Effects of Particle Shape on the Unipolar Diffusion Charging of Nonspherical Particles. *Aerosol Sci. Technol.*, 38:1045-1053.
- Olfert, J. S., Symonds, J. P. R., and Colling, N. (2007). The Effective Density and Fractal Dimension of Particles Emitted from a Light-Duty Diesel Vehicle with a Diesel Oxidation Catalyst. *J. Aerosol Sci.*, 38:69-82.
- Park, K., Cao, F., Kittelson, D. B., and McMurry, P. H. (2003). Relationship Between Particle Mass and Mobility for Diesel Exhaust Particles. *Environ. Sci. Technol.*, 37:577-583.
- Quiros, D. C., Yoon, S., Dwyer, H. A., Collins, J. F., Zhu, Y., and Huai, T. (2014). Measuring Particulate Matter Emissions During Parked Active Diesel Particulate Filter Regeneration of Heavy-Duty Diesel Trucks. *J. Aerosol Sci.*, 73:48-62.
- Quiros, D., Hu, S. H., Hu, S. S., Lee, E. S., Sardar, S., Wang, X. L., Olfert, J. S., Jung, H. J., Zhu, Y. F., and Huai, T. (2015a). Particle Effective Density and Mass During Steady-State Operation of GDI, PFI, and Diesel Passenger Cars. *J. Aerosol Sci.*, 83:39-54.
- Quiros, D., Zhang, S., Sardar, S., Kamboures, M. A., Eiges, D., Zhang M., Jung H. J., McCarthy M. J., Chan, M. C. O., Ayala, A., Zhu Y.F., Huai, T., and Hu, S. H. (2015b). Measuring Particulate Emissions of Light Duty Passenger Vehicles Using Integrated Particle Size Distribution (IPSD). *Environ. Sci. Technol.*, 49:5618-5627.
- Rubino, L., Philips, P. R., and Twigg, M. V. (2005). Measurements of Ultrafine Particle Number Emissions from a Light-Duty Diesel Engine Using SMPS, DMS, ELPI and EEPS. *SAE Technical Paper*, 2005-24-015. Society of Automotive Engineers.
- Shah, S. D., and Cocker, D. R. (2005). A Fast Scanning Mobility Particle Spectrometer for Monitoring Transient Particle Size Distributions. *Aerosol Sci. Technol.*, 39:519-526.
- Shin, W.G., Wang, J., Mertler, M., Sachweh, B., Fissan, H., and Pui, D.Y.H. (2010). The Effect of Particle Morphology on Unipolar Diffusion Charging of Nanoparticle Agglomerates in the Transition Regime. *J. Aerosol Sci.*, 41:975-986.
- Silvis, W. (2012). Measurement of In-Use PM Using Soot Augmented with a Gravimetric Reference. *SAE Technical Paper*, 2012-01-1254. Society of Automotive Engineers.
- TSI. (2013). Engine Exhaust Particle Sizer Spectrometer 3090. Available at: <http://www.tsi.com/engine-exhaust-particle-sizer-spectrometer-3090/> (accessed 9 September 2015).
- TSI. (2015). Updated Inversion Matrices for Engine Exhaust Particle Sizer (EEPS) Spectrometer Model 3090. Available at: http://tsi.com/uploaded/Files/_Site_Root/Products/Literature/Application_Notes/Updated_Inversion_Matrices_EEPS-005-A4-web.pdf (accessed 9 September 2015).
- USEPA. (2013). EPA Proposes Tier 3 Tailpipe and Evaporative Emission and Vehicle Fuel Standards. *Office of Transportation and Air Quality*, EPA-420-F-13-018a.
- Vouitsis, E., Ntziachristos, L., and Samaras A. (2008). Theoretical Investigation of the Nucleation Mode Formation Downstream of Diesel After-Treatment Devices. *Aerosol Air Qual. Res.*, 8:37-53.
- Wang, X. L., Grose, M., Caldow, R., Swason J., Watts, W., and Kittelson, D. B. (2009). Improvement of Engine Exhaust Particle Sizer Spectrometer for Engine Emissions Measurement. Presented at the 28th AAAR Annual Conference, Minneapolis, MN.
- Wang, X.L., Grose, M.A., Caldow, R., Osmondson, B.L., Swanson, J.J., Chow, J.C., Watson, J.G., Kittelson, D.B., Li, Y., Xue, J., Jung, H., and Hu, S. (Submitteda). Improvement of Engine Exhaust Particle Sizer (EEPS) Size Distribution Measurement - II. Engine Exhaust Aerosols. *J. Aerosol Sci.*
- Wang, X.L., Grose, M.A., Avenido, A., Stolzenburg, M.R., Caldow, R., Osmondson, B.L., Chow, J.C., and Watson, J.G. (Submittedb). Improvement of Engine Exhaust Particle Sizer (EEPS) Size Distribution Measurement - I. Algorithm and Applications to Compact Aerosols. *J. Aerosol Sci.*
- Wang, S. C., and Flagan, R. C. (1990). Scanning Electrical Mobility Spectrometer. *Aerosol Sci. Technol.*, 13:230-240.
- Wei, Q., Kittelson, D. B., and Watts, W. F. (2001). Single-Stage Dilution Tunnel Performance. *SAE Technical Paper*, 2001-01-0201. Society of Automotive Engineers.
- Wiedensohler, A. (1988). An Approximation of the Bipolar Charge-Distribution for Particles in the Sub-Micron Size Range. *J. Aerosol Sci.*, 19:387-389.
- Yao, X. H., Lau, N. T., Fang, M., and Chan, C. K. (2006). On the Time-Averaging of Ultrafine Particle Number Size Spectra in Vehicular Plumes. *Atmos. Chem. Phys.*, 6:4801-4807.
- Zervas, E., and Dorlhene, P. (2006). Comparison of Exhaust Particle Number Measured by EEPS, CPC, and ELPI. *Aerosol Sci. Technol.*, 40:977-984.
- Zheng, Z. Q., Durbin, T. D., Karavalakis, G., Johnson, K. C., Chaudhary, A., Cocker, D. R., Herner, J. D., Robertson, W. H., Huai, T., Ayala, A., Kittelson, D. B., and Jung, H. S. (2012). Nature of Sub-23-nm Particles Downstream of the European Particle Measurement Programme (PMP)-Compliant System: A Real-Time Data Perspective. *Aerosol Sci. Technol.*, 46:886-896.
- Zimmerman, N., Pollitt, K. J. G., Jeong, C. H., Wang, J. M., Jung, T., Cooper, J. M., Wallace, J. S., and Evans, G. J. (2014). Comparison of Three Nanoparticle Sizing Instruments: The Influence of Particle Morphology. *Atmos. Environ.*, 86:140-147
- Zimmerman, N., Jeong, C. H., Wang, J. M., Ramos, M., Wallace J. S., and Evans, G. J. (2015). A Source-Independent Empirical Correction Procedure for the Fast Mobility and Engine Exhaust Particle Sizers. *Atmos. Environ.*, 100:178-184